Morphology of Thermoplastic Polyurethanes by 1H Spin−Diffusion NMR

ARTICLE *in* MACROMOLECULES · JULY 2006

Impact Factor: 5.8 · DOI: 10.1021/ma060335m

9 AUTHORS, INCLUDING:

Mihai Adrian Voda
Unilever R&D Netherlands
24 PUBLICATIONS **185** CITATIONS
SEE PROFILE

Alina Adams Buda
RWTH Aachen University
44 PUBLICATIONS **399** CITATIONS
SEE PROFILE

Maria Baias
New York University Abu Dhabi
26 PUBLICATIONS **285** CITATIONS
SEE PROFILE

Bernhard Blümich
RWTH Aachen University
131 PUBLICATIONS **1,629** CITATIONS
SEE PROFILE

Morphology of Thermoplastic Polyurethanes by ^{1}H Spin-Diffusion NMR

Mihai A. Voda,† Dan E. Demco,† Alexandra Voda,‡ Thomas Schauber,‡ Matthias Adler,‡ Thomas Dabisch,§ Alina Adams,† Maria Baias,† and Bernhard Blümich*,†

Institut für Technische Chemie und Makromolekulare Chemie, Rheinisch-Westfälische Technische Hochschule, Worringerweg 1, D-52056 Aachen, Germany; Freudenberg Forschungsdienste KG, D-69465 Weinheim, Germany; and Merkel Freudenberg Fluidtechnic GmbH, D-34613, Germany

Received February 14, 2006; Revised Manuscript Received May 7, 2006

ABSTRACT: The morphology and domain sizes are reported for a series of thermoplastic polyurethane (TPU) samples with different content in hard segments and the same molecular weight of the soft segments. NMR spin-diffusion experiments were employed with a ^{1}H double-quantum dipolar filter to establish the dominant dimensionality of the spin-diffusion process, which is shown to take place in two and three dimensions for investigated samples. The correlation between mesoscopic and microscopic properties of the TPU samples is discussed. To this purpose the effective volume of the hard domains is correlated with the TPU content of the hard segments and the segmental orientation of the hard segments obtained from the ^{1}H residual dipolar couplings. A semiquantitative model is developed to explain the functional dependence of the residual second van Vleck moment on the effective volume of the hard segments.

1. Introduction

Many materials like polymers, composite materials, and biomaterials show microheterogeneities in both structural and associated dynamical properties. For instance, most commercial polymers are heterogeneous with properties that critically depend on the dimensional scale of the structure of the different components in the material. This is the case for partially crystalline polymers, blends and composites, segregated block copolymers, and filled and plasticized systems.[1,2] Such distributed microstructures can be probed by a variety of methods like transmission electron microscopy (TEM), field ion and atomic force microscopy (AFM), small-angle X-rays scattering, wide-angle X-rays diffraction (SAXS and WAXD), and small-angle neutron scattering (SANS). Solid-state NMR offers many techniques for characterizing heterogeneous materials at the molecular, mesoscopic, and macroscopic levels.[3−6] Moreover, an advantage of solid-state NMR methods over scattering techniques is that NMR does not require samples with long-range order.

One established NMR method to investigate domain sizes and morphology of heterogeneous polymers is based on the magnetization exchange after production of a *z*-magnetization gradient by a dipolar filter (see refs 3, 4, and 7−15 and references therein). These spin-diffusion experiments are suitable to investigate different aspects of structural heterogeneities in a broad range of spatial dimensions from 0.5 to about 200 nm.

One important class of elastomers investigated by different NMR methods is that of thermoplastic polyurethanes (TPU) (for a review see refs 16 and 17). They combine the processability of thermoplastics with rubberlike elastic properties. In most cases, segmented TPUs are regarded as multiblock copolymers of the $(AB)_n$ type, where A and B represent repeat units of the hard and soft segments. The hard segments (HS) are responsible for the dimensional stability of the TPU product by providing physical cross-links through hydrogen bonds and act as reinforcing filler to the soft segments (SS), which are responsible for the flexibility of the TPU materials. Many of the unique properties of TPU materials are greatly influenced by the phase separation of rigid and flexible segments. Thus, an estimation of the size and morphology of the domains is of considerable interest. The spin-diffusion experiment to select the mobile phase with dipolar filter and varying preparation interval was proposed by Idiyatullin et al.[11] for the study of domain morphology and sizes of polyurethane samples. This study was a continuation of the results presented by Demco et al.[10] which shows that the spin-diffusion experiment can provide information about the morphology independent of scattering methods.

In the past years, the microscopic properties of thermoplastic elastomers were investigated by solid-state NMR.[18−21] Litvinov et al.[18] investigated multiblock (poly(butylene terephthalate)-*block*-poly(tetramethylene oxide) (PTMO)) copolymers by ^{1}H and ^{13}C NMR relaxation experiments. They proved that at room temperature three different phases coexist, and the phase diagrams as well as the crystallinity of PBT were determined. Information about segmental mobility on the same systems using static ^{1}H double-quantum (DQ) NMR experiments in combination with homo- and heteronuclear dipolar filters was reported by Bertmer et al.[19] Recently, proton NMR transverse magnetization relaxation, differential scanning calorimetry (DSC), and rebound resilience (RR) techniques were used to characterize molecular chain mobility, phase composition, glass transition temperatures, and angles of rebound for a series of TPU samples.[20] In these block copolymers the molecular chains are composed of soft segments (SS) originating from the polyol and hard segments (HS) originating from the diisocyanate and the chain extender. Moreover, the segmental orientation of the same series of TPU samples with different content in hard segments and different number-average molecular weights of soft segments was investigated by ^{1}H double-quantum (DQ) NMR.[21] The correlation between the segmental orientation of

† Rheinisch-Westfälische Technische Hochschule.
‡ Freudenberg Forschungsdienste KG.
§ Merkel Freudenberg Fluidtechnic GmbH.
* To whom correspondence should be addressed: Ph +49-241-8026420; Fax +49-241-8022185; e-mail bluemich@mc.rwth-aachen.de.

10.1021/ma060335m CCC: $33.50
Published on Web 06/09/2006

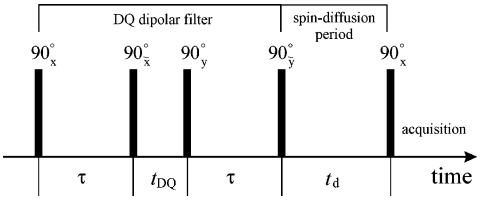

Figure 1. Scheme for the spin-diffusion experiment with a DQ filter. The first two pulses excite DQ coherences that evolve for a short time t_{DQ}. These coherences are converted by the following two pulses into *z*-magnetization. The spin diffusion takes place during the time interval of duration t_d. The last pulse reads out the distribution of magnetization between different polymer phases.

Table 1. Composition of the TPU Samples

polyol	M_n (g/mol)	mass fraction of the hard phase (%)			
Capa 2205	2000	23	36	45	54

the hard segments and the thermodynamic and mechanical properties of the TPU samples was also discussed.[21]

The aim of this work is to report the morphology and domain sizes for a series of TPU samples with different content in hard segments for the same molecular weight of the soft segments. The same set of samples has been investigated by different NMR methods and other techniques in previous studies.[20,21] The spin-diffusion experiment uses a DQ dipolar filter that allows a more accurate evaluation of the domain sizes. The dimensionality (n) of the spin-diffusion process that is connected to the sample morphology was established to be dominated by $n = 3$ for the samples with high content in hard segments. The correlation between domain sizes, TPU composition, and segmental orientation of the hard segments measured by ^{1}H residual dipolar couplings[21] is also reported.

2. Experimental Section

Polymer Synthesis. The raw materials for the preparation of the TPUs were MDI (4,4′-diphenylmethane diisocyanate) and 1,4-butanediol (BD), commercial grade purchased from Bayer. Monourethane-type mold release agent (Freudenberg Dichtungs-Schwingungstechnik K.G.) was used in a concentration of 0.5%. Difunctional polycaprolactone (PCL) was purchased from Solvay Interox under the name of Capa 2205 with molecular weight of $M_n = 2000$ g/mol. All chemicals were used as received, without any pretreatment.

In block copolymers the molecular chains are composed of SS originating from the polyol (PCL) and HS originating from the diisocyanate and the chain extender. Ideally, the two segments are immiscible and phase separate during their formation. The soft segments form the continuous soft phase in which the hard phase is dispersed. The domain size of the hard phase depends on the length of the hard segments, which can be adjusted through the mass fraction of diisocyanate and chain extender in the formulation and through the molecular weight of the polyol. The TPU samples have been prepared using the prepolymer technique. The mass fraction of the hard phase is given in Table 1. More details about the sample preparation are given in ref 20.

Proton NMR Measurements. Proton solid-state NMR spectra, DQ buildup curves and spin-diffusion data were measured on a Bruker DSX-500 spectrometer operating at 500.45 MHz for ^{1}H. The data were collected at room temperature for nonspinning samples. The dead time of the spectrometer is 5.5 μs. The length of a $\pi/2$ pulse was about 3.5 μs, the dwell time was 1 μs, and the recycle delay was 5 s for all measurements.

Proton spin-diffusion measurements were performed using the general scheme consisting of a double-quantum (DQ) dipolar filter, a spin-diffusion period, and an acquisition period as presented in Figure 1. The gradient of magnetization was created by the dipolar filter that excites DQ coherences (Figure 1) and selects mainly the magnetization of the rigid phase.[14,15] The pulse sequence is based on the two pulses acting during the excitation and reconversion periods. The value of the excitation/reconversion times is $\tau = 7$ μs. It corresponds to the rising region of the DQ buildup curve for each sample.

Table 2. Values of ^{1}H Residual van Vleck Moment $\langle M_2 \rangle$ from Ref 21 for the TPU Samples of Table 1

HS [%]	$\langle M_2 \rangle (2\pi)^2$ [kHz^2][a]
23	41
36	83
45	133
54	226

[a] The errors are of the order ±10%.

The experimental wide-line spectra were decomposed in two components using the DMFIT program.[22] The broad component of the spectra was approximated by a Gaussian function. A Lorentzian line shape was used to describe the narrow component of the spectra.

The integral area of the NMR spectra is approximately constant for the entire range of diffusion times, demonstrating that the spin−lattice processes do not significantly affect the spin-diffusion experiment. Moreover, the T_1 values of both components were determined by an inversion recovery method. The spin-diffusion process, manifested in the decay and buildup curves of the rigid and mobile components, respectively, is complete for a time scale smaller than T_1, so that no correction of the experimental data is needed. The long T_1 corresponds to the rigid component of the investigated samples. It is of the order of 1.2 s, and the short T_1 of the mobile component is longer the 400 ms.

The proton NMR DQ buildup curves provided the residual van Vleck moments. They were measured on a Bruker Minispec NMR−mq20 spectrometer at a proton resonance frequency of 20 MHz.[21] The durations of the applied pulses were 1.86 μs for the 90° pulse and 3.68 μs for the 180° pulse. The dead time of the spectrometer is 10 μs. The spectrometer was equipped with a BVT3000 variable temperature unit. The achieved temperature stability was ±0.1 °C. The NMR experiments were performed at 40 °C. When implemented on the Bruker Minispec, the pulse sequence of Figure 1 was extended by 180° refocusing pulses (of 3.68 μs length) in the middle of the excitation and reconversion periods. The DQ evolution time and the spin-diffusion delay were fixed to $t_{DQ} = t_d = 20$ μs (Figure 1). The values (Table 2) of the residual second van Vleck moments $\langle M_2 \rangle$ were obtained from the experimental data by the procedure discussed in ref 21.

3. Results and Discussion

3.1. Proton NMR Spectra and Phase Composition. Proton NMR spectra of polyurethane sample with 45% HS, recorded in static conditions, are presented in Figure 2a. The spectra have been decomposed in two components. The best fitting parameters have been found by decomposing the spectra into a Gaussian (rigid component) and a Lorentzian line (mobile component).

The phase composition of the investigated TPU samples is shown in Figure 2b as a function of theoretical content of hard segments. The measurements reveal an increasing of rigid phase with increasing the HS content in the samples, except the sample containing 23% HS. This is explained by the fact that the soft segments have massively crystallized[20] and contribute to the rigid fraction detected by NMR. This massive crystallization present only for this TPU sample is due to a very low HS content so the soft segments crystallize in order to maintain the structural stability. The measured rigid fraction from NMR spectra is smaller (Figure 2b) than the HS content except, again, the 23% HS sample. This can be explain by the editing of the free induction decay in the presence of the dead time and the massive crystallization of the sample with 23% HS.

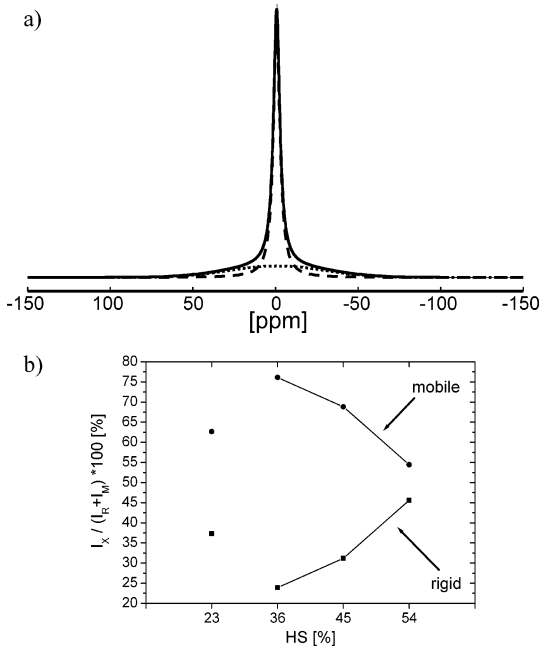

Figure 2. (a) Proton NMR spectrum of the TPU sample with 45% HS, decomposed in two components. The broad and narrow lines correspond to hard and soft domains, respectively. (b) The relative fractions of the rigid (hard) and mobile (soft) phases $I_X/(I_R + I_M)$ with X = R, M as a function of the content of HS. The continuous lines are drawn to connect the points.

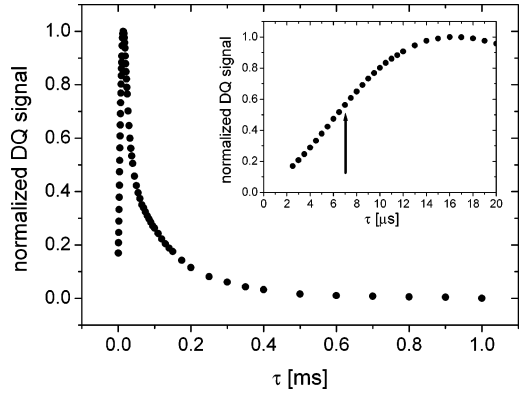

Figure 3. Proton DQ buildup curves for the TPU sample with 45% HS. The maximum corresponds to the residual dipolar couplings of the rigid phase. The DQ buildup curve does not show a second maximum corresponding to the soft segments due to the small values of the residual dipolar couplings. In the inset, the initial part of the DQ buildup curve is shown, and the arrow corresponds to the excitation/reconversion time $\tau = 7$ μs used for the DQ filter.

3.2. Double-Quantum Dipolar Filter. The spin-diffusion experiments observe the equilibration of spatially heterogeneous magnetization over the sample. To create a gradient in the magnetization, a dipolar filter which excites double-quantum (DQ) coherences can be used.[14,15] The DQ filter can be set in such a way as to select the magnetization only from the most rigid part of a heterogeneous sample. By choosing appropriate excitation/reconversion periods τ (Figure 1) of the double-quantum filter, the magnetization corresponding to the stronger dipolar couplings will pass through the filter and that of the weaker dipolar couplings is filtered out. The value of τ can be chosen by recording a DQ buildup curve as shown in Figure 3 for the sample with 45% HS, recorded using the five-pulse sequence with a filter time of $\tau = 7$ μs (Figure 1). The maxima of the DQ buildup curves appear at very short excitation/reconversion times τ below 12 μs for all investigated TPU samples. In this range of τ values, the mobile component is completely filtered out (Figure 4).

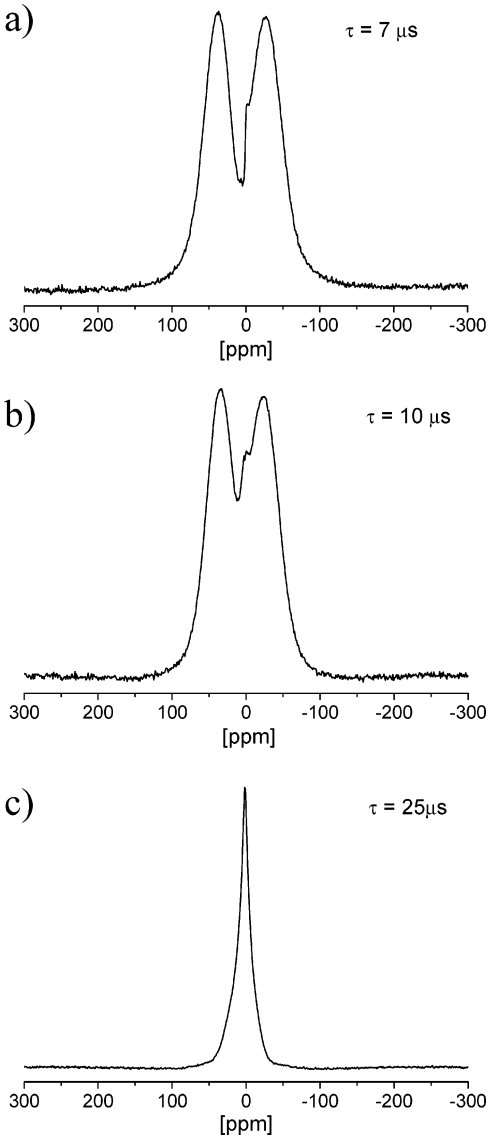

Figure 4. Proton DQ filtered spectra for different τ values measured using the pulse sequence of Figure 1 with $t_{DQ} = 5$ μs and $t_d = 5$ μs for the TPU sample with 45% HS. The NMR spectra (a)−(c) correspond to $\tau = 7$, 10, and 25 μs. The spectra shown in (a) and (b) edit the ^{1}H pairs of the hard segments. For longer values of τ, the pulse sequence acts like a filter for the mobile domains.

The DQ filtered spectra for different values of τ are shown in Figure 4. The value of 7 μs has been chosen, which still keeps the filter efficiency[10] close to unity with a reasonable value of signal-to-noise ratio. The use of this type of filter is more advantageous than a dipolar filter for mobile domains because of a more accurate detection of the narrow signals on top of the broad component compared to the detection of a broad component under a narrow signal. This is valid especially at short diffusion times when the magnetization of one of the components is very small.

3.3. Proton Spin Diffusivities. The spin-diffusion coefficients have to be evaluated in order to estimate the domain sizes of the rigid and mobile regions. Taking into account that the line shapes for the two spectral components are in a good approximation decomposed into Gaussian and Lorentzian line shapes, the spin-diffusion coefficients can be evaluated using the formalism presented in ref 10. The spin-diffusion coefficients can be expressed in terms of the local dipolar field, so that the

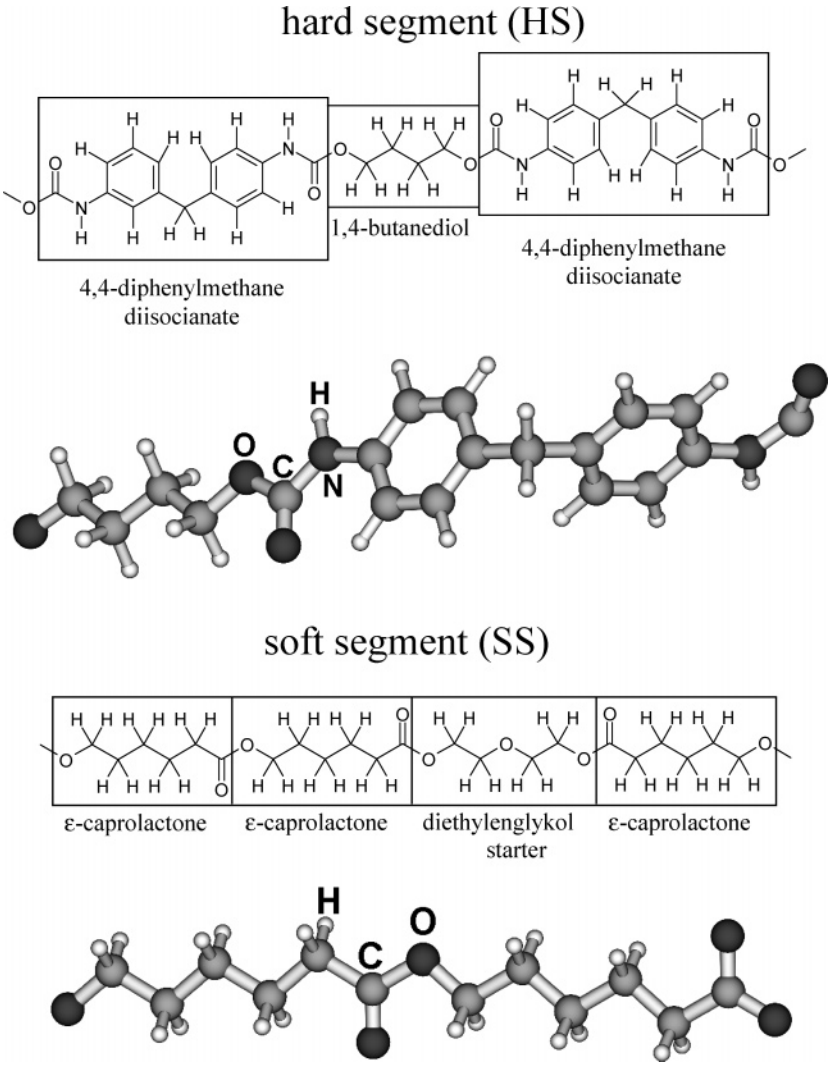

Figure 5. Optimized conformer geometry of HS (a) and SS (b) monomers derived with the help of the Gauss 03W software package. The distances between closest protons are used for evaluation of $(\langle r^2\rangle)^{1/2}$.

spin diffusivities are related to the second van Vleck moments.

The equations describing the spin-diffusion coefficients for rigid (Gaussian line) and mobile (Lorentzian line) regions are given by (see ref 10)

$$D_{\mathrm{R}} = \frac{1}{12}\sqrt{\frac{\pi}{2\ln 2}}\langle r^2\rangle \Delta\nu_{1/2} \qquad (1)$$

and

$$D_{\mathrm{M}} = \frac{1}{6}\langle r^2\rangle [\alpha\Delta\nu_{1/2}]^{1/2} \qquad (2)$$

where α is the cutoff parameter of the Lorentzian line, $\Delta\nu_{1/2}$ is the full line width at half-height, and $\langle r^2\rangle$ is the mean-square distance between the nearest spins.

Taking into account the complexity of the chemical structure and the large number of protons in the TPU samples, the $\langle r^2\rangle$ value has been computed by molecular optimizations for both hard and soft segments by the Gaussian 03W software package (Gaussian Inc., Pittsburgh PA, 2003).[22] The molecular optimization is based on the density functional theory (DFT) methods. For the geometry optimizations we used the three-parameter hybrid exchange functional[23] combined with LYP (Lee, Yang, and Parr)[24] correlation (referred to as B3LYP) and the 6-31G-(d) basis set (six Gaussians for 1s, three Gaussians for the inner 2s, and 2p, and one Gaussian for the outer 2s, and 2p orbitals). For the samples under investigation the computation time was about 3 days for each, hard and soft segments, on a Pentium IV computer equipped with a CPU working at 2.6 GHz and a DDR type memory of 2 GB. The result of the optimization is shown in Figure 5, and the averaged $\langle r^2\rangle^{1/2}$ values obtained for HS and SS are 0.37 and 0.29 nm, respectively.

Table 3. Full Width at Half-Intensity $\Delta\nu_{1/2}$ Obtained from the Components of ^{1}H NMR Spectra of TPU Samples with the Composition Shown in Table 1

HS [%]	Gaussian component $\Delta\nu_{1/2}$ [kHz]	Lorentzian component $\Delta\nu_{1/2}$ [kHz]
23	33.7	2.3
36	27.6	2.1
45	31.1	2.3
54	32.0	2.7

Proton spin diffusivities of rigid and mobile phases for the TPU samples were evaluated using eqs 1 and 2, and the line widths are reported in Table 3. The spin diffusivities are shown in Figure 6 as a function of the content in hard segments. The strength of the ^{1}H residual dipolar couplings increases in the regions of HS and SS with the increase in the content of HS.[20,21] Therefore, the spin diffusivities will increase in both phases when the concentration in HS increases, as is evident from Figure 6a.

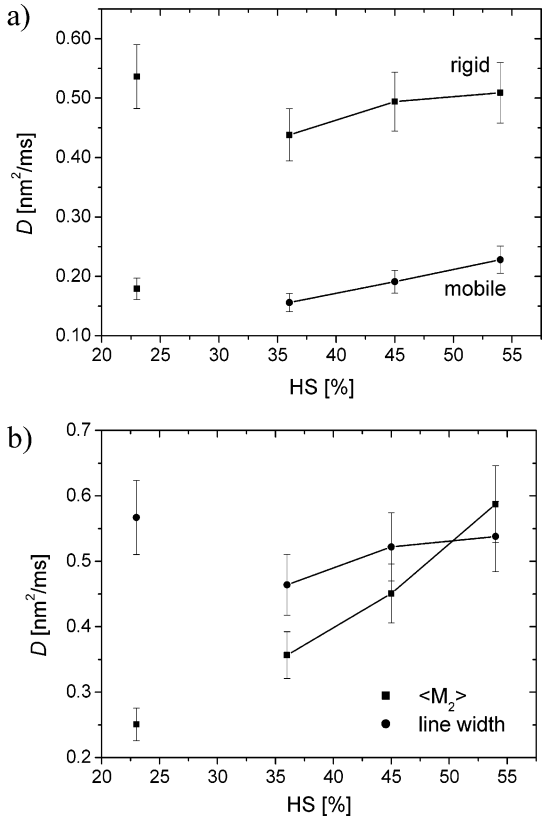

Figure 6. (a) Proton spin diffusivities for rigid and mobile domains vs % HS evaluated from the line width using eqs 1 and 2. (b) Comparison of the spin diffusivities of the rigid domain evaluated from the $\langle M_2 \rangle$ (squares) and line width (circles).

The spin diffusivity of the rigid phase in TPU samples can be evaluated by the second approach. This approach is independent of that based on the measurements of the line widths (see above). The starting point is based on the relationship between the spin diffusivity of the quasi-rigid-phase D_R and the local dipolar field B_L for a powder sample,[25] i.e.

$$D_R = \sqrt{\frac{\pi}{60}} \langle r^2 \rangle B_L \tag{3}$$

For purely dipolar spin interactions, the local field is related to the residual second van Vleck moment $\langle M_2 \rangle$ by the relation[26]

$$B_L = \sqrt{\frac{5}{3}} \langle M_2 \rangle \tag{4}$$

From eqs 3 and 4 we obtain

$$D_R = \frac{\sqrt{\pi}}{6} \langle r^2 \rangle \langle M_2 \rangle \tag{5}$$

The measurements of the residual second van Vleck moment using DQ buildup curves were reported in ref 21 and the resultant values are summarized in Table 2. The values of the spin diffusivities for the rigid phase of the TPU samples evaluated by both approaches discussed above are compared in Figure 6b. The values of D_R evaluated from the measurements of $\langle M_2 \rangle$ differ from the values estimated from the line widths by about 10−20%. The only sample showing large differences between both spin diffusivities is the sample with 23% HS. This can be explained by the differences in editing strong dipolar couplings by NMR spectra and DQ coherences. In the last case only the strongest dipolar couplings from HS are edited. In the former case the crystallized SS as well as rigid HS are edited by the NMR spectrum. Because the spin-diffusion experiments are performed using the DQ dipolar filter, the spin-diffusivities evaluated from $\langle M_2 \rangle$ are used in the simulation of the experimental data.

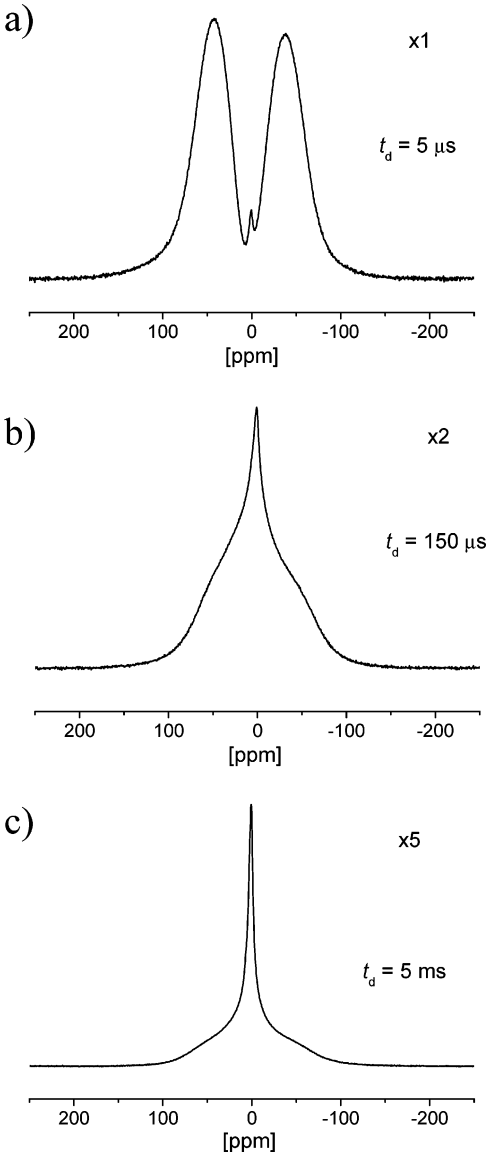

Figure 7. Proton spin-diffusion edited NMR spectra at different diffusion times $t_d = 5$ μs (a), $t_d = 150$ μs (b), and $t_d = 5$ ms (c) for 45% HS TPU sample.

3.4. Dominant Morphology and Effective Domain Sizes. Proton spectra recorded after different diffusion times using the DQ filter (cf. Figure 1) are shown in Figure 7 for the TPU sample with 45% HS. In all cases the flow of longitudinal magnetization from the rigid domain into the mobile domain is observed with increasing diffusion times. For all TPU samples, the equilibration of the magnetization takes place on a time scale smaller than the relaxation of the longitudinal magnetization; hence, a correction of the spin-diffusion data corresponding to the relaxation effects has not been performed.

The time-dependent integral spin-diffusion intensities obtained for the TPU sample with 45% HS are plotted in Figure 8. The quasi-equilibrium is reached in about 200 ms. In a good approximation, the spin-diffusion edited ^{1}H NMR spectra can be decomposed in two components. These data can be used for establishing the dominant morphology and the average domain sizes.

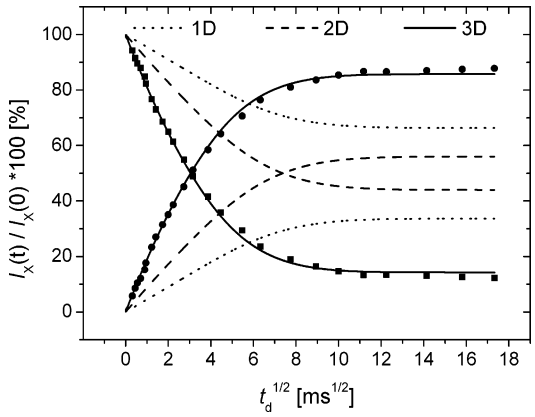

Figure 8. Proton spin-diffusion decay and buildup curves $I_X(t)/I_X(0)$ (X = R, M) for the 45% HS TPU sample. The lines correspond to the fits with 1D, 2D, and 3D solutions of the spin-diffusion equations (Appendix A).

The ability of NMR spin-diffusion experiments to provide self-consistent information on the dimensionality of the diffusion process, average phase domain sizes, and the details of the phase morphology has been analyzed theoretically and validated with experimental data for a semicrystalline polymer in ref 10. It was shown that the solutions of the spin-diffusion equations for different morphologies exhibit different sensitivity to the dimensionality of the process as a result of different contact interface area for a given source volume.

For simplicity, we assume that the hard domains are surrounded by the soft domains (hereafter SS/HS/SS morphology). This is a plausible morphology for our TPU samples with relatively large values of the molar mass of the soft segments. We note that this is not the case for some segmented polyurethane samples, especially with low SS concentration. In this case the domains of the soft segments are surrounded by hard segments.[11] The most simple structural units for the cases of 1D, 2D, and 3D spin diffusion for a SS/HS/SS morphology are shown in Figure 9. The initial localization of the magnetization produced by the DQ dipolar filter is shown by gray and belongs to the HS phase.

Using simple geometrical arguments in the approximation of two phases, the following equations can be derived:

$$\frac{rE}{p} = 1, \quad \text{1D case}$$

$$\frac{rE}{p(2+p)} = 1, \quad \text{2D case}$$

$$\frac{rE}{(1+p)^3 - 1} = 1, \quad \text{3D case} \qquad (6)$$

where $r = \rho_R/\rho_M$ and $E = M_{M,eq}/M_{R,eq}$. The equilibrium magnetizations for the mobile (SS) and rigid (HS) domains are denoted $M_{M,eq}$ and $M_{R,eq}$, respectively. The ratio between the domain sizes d_M and d_R (cf. Figure 9) is denoted $p = d_M/d_R$.

In the following, the most probable dimensionality for the spin-diffusion process is discussed for the TPU sample with 45% HS. The same results are obtained also for the TPU samples with high content in HS i.e., 36% and 54%. For this sample the quantities r and E have the values $r = 0.85$ and $E = 2.23$. These values are established independent of the spin-diffusion process. The spin-diffusion decay and buildup curves shown in Figure 8 were fitted with the solutions of the spin-diffusion equations for 1D, 2D, and 3D morphologies. For the last two cases these were taken as a product of 1D spin-diffusion solutions (see Appendix A and Figure 9). For each spin-diffusion dimensionality the values of d_M and d_R were established from the best fit. These values were used to estimate the ratio p and finally the ratios given by eqs 6. These ratios are shown in Table 4. The ratio with the value closer to unity corresponds to the 3D morphology. The morphology of the TPU samples under investigation with high HS content is different from that found by Idiyatullin et al.[11] in TPU samples obtained by copolymerization of poly(diethylene glycol) adiapte as soft blocks with 2,4-tolylene diamine and 2,4-toluene diisocyanate as hard blocks.

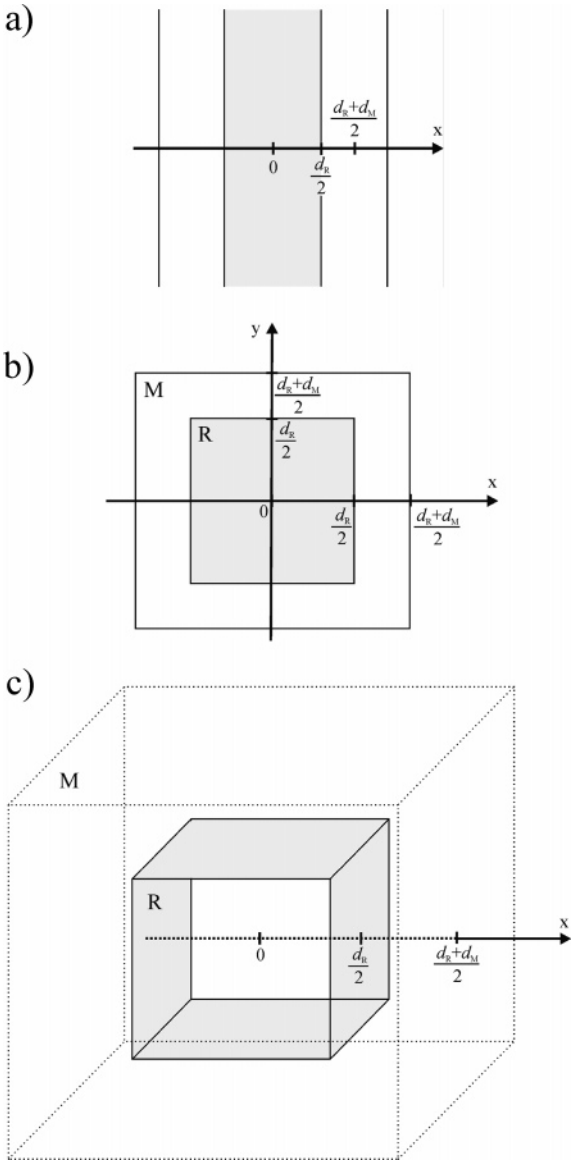

Figure 9. Morphological units for the 1D (a), 2D (b), and 3D (c) spin diffusion. The domain sizes for the rigid and mobile phases are d_R and d_M, respectively. The source of magnetization is considered to be in the rigid region (gray).

Table 4. Sensitive Ratios of the Spin-Diffusion Dimensionality (Cf. Eq 6) for TPU Samples with 23% HS and 45% HS

dimensionality ratio	values of the dimensionality ratio (23% HS)	values of the dimensionality ratio (45% HS)
1D		
rE/p	0.79	1.79
2D		
$rE/[p(2+p)]$	0.92	1.13
3D		
$rE/[(1+p)^3 - 1]$	0.83	1.02

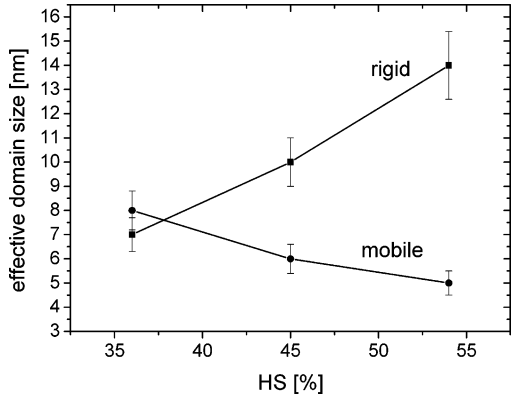

Figure 10. Effective domain sizes for rigid (squares) and mobile (circles) phases as a function of the HS content. Only the data of the TPU samples with the high HS content are shown.

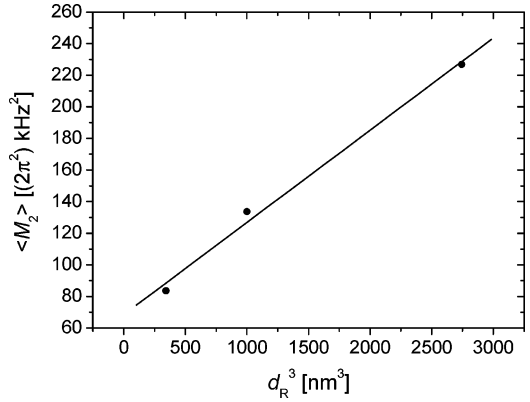

Figure 11. Correlation between the residual second van Vleck moments $\langle M_2 \rangle$ (Table 2) and the effective volume d_R^3 of the HS domains. The solid line corresponds to the best fit of the data.

In the latter case a 2D morphology was detected by spin-diffusion experiments with a variable Goldman-Shen filter.[11] This morphology describes better the samples with a low HS concentration of 23%. For this TPU sample, following the procedure discussed above, the morphology ratios in eqs 6 are given in Table 4. The two-dimensional morphology is found to be most probable.

The morphology of segmental TPU with low concentration of hard segments was investigated by atomic force microscopy (AFM) and X-ray scattering.[27,28] In general, there are two different types of dispersed HS morphologies: (1) fibrillar domains in which the domain axes coincide with the polymer chain axes and (2) the lamellar domains in which the domain axes are perpendicular to the polymer axes. This last morphology is found from the spin-diffusion experiments for the TPU sample with 23% HS. Moreover, a recent investigation[29] of polyurethane with AFM suggests two levels of hierarchy: (1) the hard segments form lamellae of about 10 nm width and (2) assemblies of these hard domains which form larger microdomains of about 100−400 nm in length and about 50 nm in width. Our spin-diffusion experiments do not probe this hierarchy due to a faster equilibration of the magnetization gradient on the scale of tenth of nanometers.

In TPU samples with higher HS content where more continuity of the hard-segment phase would exist, the morphology is expected to be different for that of the samples with low concentration in HS. Therefore, a 3D morphology is expected to be most probable, in agreement with the results obtained from ^{1}H spin-diffusion experiments.

The domain sizes for TPU samples with higher HS content were evaluated from the spin-diffusion decay and buildup curves in terms of 3D morphologies represented by cubic HS domains surrounded by cubic SS domains (Figure 9). This assumption is of course a strong approximation of the reality but allows us to estimate an *effective* size of the domains which can be correlated with the chemical composition and other material properties. The effective domain sizes for rigid (HS) and mobile (SS) phases obtained by using eqs A1−A3 with $n = 3$ are shown in Figure 10 as a function of HS concentration. As expected, the effective sizes of rigid and mobile domains change linearly with the HS content for the samples rich in HS and have opposite slopes.

3.5. Correlation between Effective Domain Sizes and the Residual Dipolar Couplings. The domain sizes characterize the materials on the mesoscopic scales, i.e., on the scale of tenth of nanometers as in the case of TPU samples. The values of proton residual dipolar couplings for hard segments correlate with the anisotropic orientation of the polymer segments and reflect the property of the materials on the nanoscale. Larger values of the residual dipolar couplings mean inter alia slower segmental motions due to more dense packing, higher chain orientations produced by the influence of the soft segments, and an increase in the extend and strength of the effective dipolar network due to the interchain couplings.

Even if the quantities discussed above characterize the materials on different length scales, a correlation between the ^{1}H residual second van Vleck moments of TPU samples and the effective volume of HS domain sizes can be established. This is shown in Figure 11. The increase in the ^{1}H residual dipolar couplings shows a monotonic dependence on the effective domain volumes of the hard segments. A semiquantitative explanation for this functional dependence can be given. The residual second van Vleck moment can be written as $\langle M_2 \rangle = S^2 M_{2,\mathrm{rigid}}$, where S is the dynamic order parameter and $M_{2,\mathrm{rigid}}$ is the second van Vleck moment for a rigid dipolar network.[16] The last quantity depends on the lattice sum $\sum_k (1/r_{jk}^6)$, where r_{jk} is the internuclear distance between the spins j and k. The lattice sum increases with the number of spins k coupled by dipolar interactions with the spin j. To prove that, let us consider a continuous distribution of spins distributed uniformly in a sphere of radius R and volume V. The initial radius of the sphere is R_0, and the volume is V_0. The lattice sum can be evaluated by the approximation

$$\sum_k \frac{1}{r_{jk}^6} \propto \int_{R_0}^{R} \frac{1}{r^6} r^2 \, \mathrm{d}r \int_0^{2\pi} \mathrm{d}\phi \int_0^{\pi} \sin\theta \, \mathrm{d}\theta \tag{7}$$

Finally, we obtain

$$\sum_k \frac{1}{r_{jk}^6} \propto \frac{|V - V_0|}{V_0 V} \tag{8}$$

The above equation shows that when the volume of the dipolar network increases, i.e., $V > V_0$, the lattice sum becomes larger and $M_{2,\mathrm{rigid}}$ increases. This variation is not linear in the volume of the dipolar network, as is shown by eq 8.

To establish the dependence of residual second van Vleck moment on the effective volume of the hard segments in TPU, we have to consider also the behavior of the dynamic order parameters. Increased segmental orientation is induced by packing effect and larger hindrances of segmental motions. A very simple model is discussed in Appendix B to mimic these complex effects. On the basis of this model, we obtain $S^2 \propto a$

$-bV^2$ (eq B1), where a and b are constants. From eq 8 and eq B1 we can write finally

$$\langle M_2 \rangle \propto \frac{a}{V_0} + bV \tag{9}$$

for $V < V_0$. In the limit of the above crude models, the residual second van Vleck moment shows a linear dependence on $V \propto d_R^3$. The data in Figure 11 can be fitted in a good approximation by a straight line in accordance with eq 9. The data of the "pathological" TPU sample with 23% HS are excluded from all the plots of Figures 10 and 11.

4. Conclusions

Morphology and domain sizes for TPU samples with constant molar mass for the soft segments and variable content in the hard segments were investigated by ^{1}H spin-diffusion experiments in the approximation of the rigid and mobile domains. The rigid domains are associated with the hard segments and the mobile domains with the soft segments. In a good approximation, the ^{1}H NMR spectra can be decomposed in two components showing that, for the investigated TPU samples, the mixed phase can be incorporated in the mobile phase.

The most probable morphology is three-dimensional for the TPU samples with a high content in HS and was established by a combination between the equilibrium magnetizations and the domain size ratios obtained from simulations of the spin-diffusion process using 1D, 2D, and 3D solutions of the spin-diffusion equations. In these simulations, the hard segments were considered to be embedded in the soft segments. For other molar masses of SS and different HS contents, this morphology can be inverted. The effective domain size of the rigid phase increases with the content in the hard segments showing an extended spatial organization. This takes place at the expense of the domain sizes for the soft domains. Proton spin diffusivities increase for both phases due to the enhanced hindering in the segmental mobility. This effect is induced by the increase in the HS content.

The segmental orientation represents a microscopic property of the polymer. Quantitatively, this is described by the residual second van Vleck moment. This NMR parameter can be correlated with the spatial extension of the dipolar network and the restriction of segmental motions induced by the chain packing. A simple, semiquantitative model was developed to explain the linear dependence of $\langle M_2 \rangle$ on the effective volume d_R^3 of the hard segments.

The correlation of macroscopic, mesoscopic, and microscopic material parameters can be used to gain a deeper understanding of the behavior of many classes of heterogeneous polymers including nanocomposites. The results of this work stress the importance of the mesoscopic information in this endeavor.

Acknowledgment. Financial support of this project by the Deutsche Forschungsgemeinschaft (DE 780/2-1) is gratefully acknowledged. Alexandra Voda acknowledges Freudenberg Forschungsdienste KG (Physical Testing Department) for financial support of her PhD work.

Appendix A

We assume that the spin diffusion takes place in a heterogeneous polymer from a source R with low segmental mobility into a finite sink M with larger segmental mobility. The presence of an interface is neglected in the following considerations. The relationships describing the time evolution of the integral intensities of the NMR signals $I_R(t)$ and $I_M(t)$ for a spin-diffusion process of dimensionality n ($n = 1$, 2, and 3) can be obtained from refs 12 and 15. The spin magnetization in the source region (R) for an n-dimensional spin-diffusion process is given by

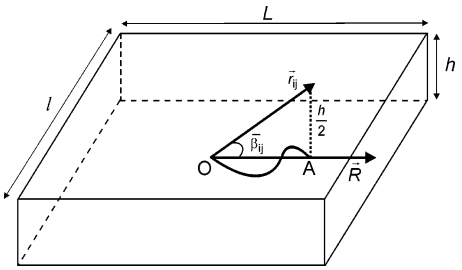

Figure 12. Geometrical model used for modeling the effect of packing and hindrance in segmental motions on the dynamic order parameter. The two faces of the rectangle separated by the distance h act as barriers which increase the value of S. The internuclear vector is $\vec{r}_{ij}$, $\bar{\beta}_{ij}$ is the average azimuthal angle, and $\vec{R}$ is the end-to-end vector.

$$I_R(t) \approx \rho_R[2\int_0^{d_R/2} m_R(x,t)\,dx]^n \tag{A1}$$

where ρ_R is the number density of spins of the source R of size d_R and $m_R(x,t)$ is the space- and time-dependent concentration of the z spin magnetization. For a dipolar filter that selects only the magnetization of the R region, the spin magnetization in the sink region can be written as

$$I_M(t) = I_R(0) - I_R(t) \tag{A2}$$

The quantity $m_R(x,t)$ is given by[12]

$$m_R(x,t) = \frac{\rho_R d_R m_{0R}}{\rho_R d_R + \rho_M d_M} - \sum_{m=1}^{\infty} 2m_{0R} \sin[kd_M\beta_m] \cos[x\beta_m] \exp[-D_R\beta_m^2 t]\beta_m^{-1}\{[\sigma d_R + kd_M] \cos[d_R\beta_m] \cos[kd_M\beta_m] - [\sigma k d_M + d_R] \sin[d_R\beta_m] \sin[kd_M\beta_m]\}^{-1} \tag{A3}$$

where d_M is the size of the sink, ρ_M is the number density of spins in the region M, $k = (D_R/D_M)^{1/2}$, and $\sigma = k\rho_R/\rho_M$. The spin-diffusion coefficients in the regions R and M are denoted by D_R and D_M, respectively. The quantities β_m ($m = 1$, 2, 3, ...) are the roots of a trigonometric equation defined in ref 12.

Appendix B

The dynamic order parameter is given by $S = \bar{P}_2(\cos\beta_{ij}(t))$, where $\beta_{ij}(t)$ is the instantaneous angle between a given internuclear vector $\vec{r}_{ij}$ and end-to-end vector $\vec{R}$. The time average is denoted by a bar for the second-order Legendre polynomial $P_2(\cos\beta_{ij}(t)) = {}^1/_2(3\cos^2\beta_{ij}(t) - 1)$.

The increase in the volume of the HS in TPU samples will lead to packing effects and hindrance in the segmental motions. The consequences of these complex effects on the dynamic order parameter are difficult to describe quantitatively. To mimic these effects, we consider a geometrical model shown in Figure 12. The internuclear vector $\vec{r}_{ij}$ is limited in its angular motion due to segmental motions by the walls of a rectangle separated by the distance h (Figure 12). The time average of the Legendre polynomial is replaced by an average azimuthal angle $\bar{\beta}_{ij}$. On the basis of this assumption from simple geometrical considerations (see Figure 12), we can write

$$S^2 \propto a - bV^2 \tag{B1}$$

where $a = 1$ and $b = 3/(8L^2l^2r_{ij}^2)$. The effective volume that restrict the motions of the internuclear vector is $V = Llh$. The above equation is written in the approximation $r_{ij} > h/2$. In agreement with eq B1, the dynamic order parameter increases when the volume V becomes smaller.

References and Notes

(1) Cowie, J. M. G. *Polymers: Chemistry & Physics of Modern Materials*; Blackie Academic & Professional: Glasgow, 1996.
(2) Hamley, I. W. *The Physics of Block Copolymers*; Oxford University Press: Oxford, 1998.
(3) McBrierty, V. J.; Packer, K. J. *Nuclear Magnetic Resonance in Solid Polymers*; Cambridge University Press: Cambridge, 1993.
(4) Schmidt-Rohr, K.; Spiess, H. W. *Multidimensional Solid-State NMR and Polymers*; Academic Press: London, 1994.
(5) Blümich, B. *NMR Imaging of Materials*; Clarendon Press: Oxford, 2000.
(6) Demco, D. E.; Blümich, B. *Concepts Magn. Reson.* **2000**, *12*, 188 and 269.
(7) Goldman, M.; Shen, L. *Phys. Rev.* **1966**, *144*, 321.
(8) Clauss, J.; Schmidt-Rohr, K.; Spiess, H. W. *Acta Polym.* **1993**, *44*, 1.
(9) VanderHart, D. L.; McFadden, G. B. *Solid State Nucl. Magn. Reson.* **1996**, *7*, 45.
(10) Demco, D. E.; Johansson, A.; Tegenfeldt, J. *Solid State Nucl. Magn. Reson.* **1995**, *4*, 13.
(11) Idiyatullin, D. Sh.; Khozina, E. V.; Smirnov, V. S. *Solid State Nucl. Magn. Reson.* **1996**, *7*, 17.
(12) Wang, J. *J. Chem. Phys.* **1996**, *104*, 4850.
(13) Hu, W.-G.; Schmidt-Rohr, K. *Polymer* **2000**, *41*, 2979.
(14) Buda, A.; Demco, D. E.; Bertmer, M.; Blümich, B.; Litvinov, V. M.; Penning, J.-P. *J. Phys. Chem. B* **2003**, *107*, 5357.
(15) Buda, A.; Demco, D. E.; Bertmer, M.; Blümich, B.; Reining, B.; Keul, H.; Höcker, H. *Solid State Nucl. Magn. Reson.* **2003**, *24*, 39.
(16) Demco, D. E.; Hafner, S.; Spiess, H. W. *Handbook of Spectroscopy of Rubbery Materials*; Shawbury, V. M., De Litvinov, P. P., Eds.; Rapra Technology Ltd., U.K., 2002.
(17) Demco, D. E.; Blümich, B. *Encycl. Polym. Sci. Techn.* **2004**, *10*, 637−685.
(18) Litinov, V. M.; Bertmer, M.; Gasper, L.; Demco, D. E.; Blümich, B. *Macromolecules* **2003**, *36*, 7598−7606.
(19) Bertmer, M.; Gasper, L.; Demco, D. E.; Blümich, B.; Litvinov, V. M. *Macromol. Chem. Phys.* **2004**, *205*, 83−94.
(20) Voda, A.; Beck, K.; Schauber, T.; Adler, M.; Dabisch, T.; Bescher, M.; Viol, M.; Demco, D. E.; Blümich, B. *Polym. Test.* **2006**, *25*, 203−213.
(21) Voda, A.; Voda, M. A.; Beck, K.; Schauber, T.; Adler, M.; Dabisch, T.; Besher, M.; Viol, M.; Demco, D. E.; Blümich, B. *Polymer* **2006**, *47*, 2069−2079.
(22) Massiot, D.; Fyon, F.; Capron, M.; King, I.; Le Calvé S.; Alonso, B.; Durand, J.-O.; Bujoli, B.; Gan, Z.; Hoatson, G. *Magn. Reson. Chem.* **2002**, *40*, 70−76.
(23) Becke, A. D. *J. Chem. Phys.* **1993**, *98*, 5648.
(24) Lee, C.; Yang, W.; Parr, R. G. *Phys. Rev. B* **1988**, *37*, 785.
(25) Cheung, T. T. P. *Phys. Rev. B* **1981**, *37*, 1404.
(26) Goldman, M. *Spin Temperature and Nuclear Magnetic Resonance in Solids;* Clarendon Press: Oxford, 1970.
(27) McLean, R. S.; Sauer, B. B. *Macromolecules* **1997**, *30*, 8314.
(28) Yeh, F.; Hsiao, B. S.; Sauer, B. B.; Michel, S.; Siesler, H. W. *Macromolecules* **2003**, *36*, 1940.
(29) Zheng, J.; Ozisik, R.; Siegel, R. W. *Polymer* **2005**, *46*, 10873.

MA060335M